

DSN Water Vapor Radiometer—Tropospheric Range Delay Calibration

S. D. Slobin and P. D. Batelaan
Radio Frequency and Microwave Subsystems Section

This report discusses the calibration of the DSN water vapor radiometer by means of simultaneous antenna temperature and radiosonde measurements at Edwards Air Force Base. The calibration of radiometer gain and hot load radiometric noise temperature is also described. Calibration equations are given. It is found that with a selected data set, the RMS error is less than 1 cm over a total delay range of 9 to 38 cm. Limitations on the use of the water vapor radiometer are also given.

I. Introduction

During August and December 1977 a series of water vapor radiometer (WVR) system tests were made at Edwards Air Force Base (EAFB), about 80 km (50 mi) north of Los Angeles, in the Mojave Desert. Radiosondes (RWS) were launched there daily, and simultaneous WVR microwave measurements were made at 22.235 and 18.5 GHz. Radiosondes report the temperature, pressure, and relative humidity in flight along some basically vertical path through the atmosphere up to an altitude of about 6 to 9 km (20,000 to 30,000 ft) at EAFB. They are capable of reaching altitudes of 30 km (100,000 ft), but since virtually all atmospheric water vapor resides below 6 km (20,000 ft), higher altitude reporting is not necessary for the purpose of WVR calibration of water vapor-induced tropospheric range delay.

Tipping curve measurements (antenna temperature vs elevation angle) were used to calibrate the radiometric noise temperature of the heated waveguide reference termination (hot load).

With a calibrated hot load, absolute determinations of antenna temperature were made using the ambient and hot

loads as calibration points. When corrections for cosmic and oxygen contributions were made, the resulting "water" (vapor plus liquid) noise temperatures were used to develop a second-order regression expression linking WVR noise temperature measurements and RWS-derived tropospheric delay determinations. Liquid water refers to clouds only, not rain. The WVR is not expected to be operated during rain.

Previous water vapor radiometer development has been reported in Refs. 1 and 2.

II. Theoretical Basis of Calibration

General descriptive expressions for brightness temperature in terms of precipitable¹ water vapor and liquid water can be written (Refs. 3 and 4):

¹Precipitable water is the amount or depth of water along a particular path that would lie on the ground in liquid form if it were removed from moist air or clouds. It has the units g/cm² or cm.

$$T_{22.235} = \underbrace{2.7}_{\text{cosmic}} + \underbrace{3.8m}_{\text{oxygen}} + \underbrace{16M_V}_{\text{vapor}} + \underbrace{237M_L}_{\text{liquid}} \quad (1)$$

$$T_{18.5} = 2.7 + 3.0m + 4.416M_V + 164M_L \quad (2)$$

where

T = antenna temperature at the given frequency

m = number of air masses through which the antenna looks; e.g., $m = 2$ at 30-deg elevation angle

M_V = precipitable water vapor along antenna beam, cm

M_L = precipitable liquid water along antenna beam, cm

Typical values used in this expression are:

$M_V = 1.2 \text{ g/cm}^2 \text{ (cm)}$ along a vertical path for a surface density of 7.5 g/m^3 and a scale height² of 1.6 km above the ground

$M_L = 0.1 \text{ g/cm}^2 \text{ (cm)}$ along a vertical path for a dense cloud (1 g/m^3) 1 km thick

16 = water vapor emission coefficient as determined in Ref. 4 by integrating radiosonde runs at Tuscon, Arizona (K/g/cm^2)

16/4.416 = ratio of water vapor attenuation (emission) at 22.235 and 18.5 GHz, respectively

237 = K/g/cm^2 from emission calculations using a particular cloud model (Refs. 5 and 6)

237/164 = (frequency)² attenuation relationship in liquid water clouds (Refs. 5 and 6).

Whereas the vapor coefficients can be determined with fair accuracy (10 percent) from radiosonde measurements and integration of the equation of radiative transfer, the liquid coefficients may be in error by an order of magnitude, as they are based on assumptions of the values of "unmeasurables," such as the index of refraction of an inhomogeneous distribution of liquid water particles with unknown size distribution (1 to 50 microns radius).

Tropospheric range delay can be determined theoretically and experimentally as a function of precipitable vapor and liquid (Refs. 3 and 4):

$$\begin{aligned} \Delta L &= 6.1 M_V + 1.6 M_L \\ &= 7.32 + 0.16 = 7.48 \text{ cm for the typical} \\ &\quad \text{values given above} \end{aligned} \quad (3)$$

²Scale height is that height above the ground where the water vapor density has decreased to $1/e$ of its surface value, assuming an exponential distribution of density.

It is seen that even a dense cloud has a small effect on range delay when compared to the effect of a normal water vapor distribution. The principal confusing aspect of liquid water is its large contribution to antenna temperature without a corresponding effect on range delay. The two-frequency atmospheric probing technique allows the separation of vapor and liquid effects.

Manipulation of the previous equations allows one to solve for range delay and precipitable water in terms of "water" noise temperature, where the "water" noise temperature is inferred from measurements of antenna temperature:

$$\Delta L = 0.624T_{W22} - 0.899T_{W18} \quad (4)$$

where T_{W22} and T_{W18} are water noise temperatures at 22.235 and 18.5 GHz, with typical values of 42.9 K and 21.7 K, respectively, for the vapor and liquid (cloud) combination described above.

$$\begin{aligned} M_V &= 0.103 T_{W22} - 0.150 T_{W18} \\ &= 1.2 \text{ g/cm}^2 \text{ (cm) typically for vapor} \end{aligned} \quad (5)$$

$$\begin{aligned} M_L &= -0.00273T_{W22} + 0.0101T_{W18} \\ &= 0.1 \text{ g/cm}^2 \text{ typically for liquid} \end{aligned} \quad (6)$$

The solution for zenith range delay in terms of zenith antenna temperatures is:

$$\Delta L = 1.034 + 0.624T_{22} - 0.899T_{18} \quad (7)$$

where the T 's are antenna temperatures measured at zenith only. Note that the coefficients of the temperature terms remain the same.

Figure 1 shows a plot of Eq. (4) in the region of validity (the tilted triangular region):

$$\begin{aligned} \Delta L &> 0.0 \\ T_{W18} &< 0.687T_{W22} \text{ (liquid only, } M_V = 0.0) \\ T_{W18} &> 0.270T_{W22} \text{ (vapor only, } M_L = 0.0) \end{aligned}$$

In the vapor-only condition, all data points would lie along the edge of the plane defined by the line:

$$\Delta L = 0.624T_{W22} - 0.899T_{W18} \quad (8)$$

where $T_{W18} = 0.270T_{W22}$.

The liquid-only condition results in data points lying along the line:

$$\Delta L = 0.624T_{W22} - 0.899T_{W18} \quad (9)$$

where $T_{W18} = 0.687T_{W22}$. Delay values for this condition are small, approximately 0.6 cm for water noise temperatures of 100 K and 68.7 K at 22.235 and 18.5 GHz, respectively.

The real world operates with antenna temperatures which show a condition known as “saturation.” In this case, the antenna temperatures do not rise as rapidly as increasing amounts of vapor and liquid. Indeed, infinite amounts of atmospheric water would result in antenna temperatures at both frequencies “saturated” at approximately 290 K. Graphically, the saturation effects may be shown as in Fig. 2, where the calibration plane shows an upward curvature—the delay rising faster than the temperature. Alternatively, the plane may be allowed to remain flat and the temperature axes stretched to accommodate the saturation effects.

Clearly, the calibration of the WVR must entail defining the bounded curved plane. Data should be taken under a variety of weather conditions to accurately define the surface. It should be remembered at this point that the examples given previously are for illustrative purposes and only approximately and occasionally represent values obtained by experiment.

III. Airmass Correction for Antenna Beamwidth

The WVR horn antenna has a moderately wide 3-dB beamwidth, 7 deg (± 3.5 deg) at 22.235 GHz and 9 deg (± 4.5 deg) at 18.5 GHz. Because of this, the net airmass through which the antenna looks is not given by the classic cosecant (elevation angle), even though the flat-earth assumption is made in this analysis. The lower half of the beam weights the pointing more than the upper half, so that electrically the antenna points lower than the geometric axis of the horn. For tipping curve analysis, the net airmass through which the antenna looks must be calculated.

This is done by integrating over the antenna beam:

$$\langle CSC(EL) \rangle = \frac{\int \int CSC(EL) G(\theta, \phi) dA}{\int \int G(\theta, \phi) dA} \quad (10)$$

where

EL = elevation angle

$G(\theta, \phi)$ = horn pattern gain

The results for particular angles are shown in Table 1.

For ease of calculation, the following expressions approximate the airmass values (m) in Table 1 for elevation angles greater than 30 deg:

$$m = (1/\sin EL)^{1.025} \text{ for 22.235 GHz}$$

$$m = (1/\sin EL)^{1.035} \text{ for 18.5 GHz} \quad (11)$$

EL = elevation angle of horn axis

Alternate expressions may be used for elevation angles less than 30 deg.

IV. Hot Load Calibration

The start of the WVR calibration sequence is to do a series of tipping curves, where noise temperature measurements (data counts) are made looking at the sky at elevation angles from zenith (one air mass) down to about 15 deg (4 air-masses). When these data are extrapolated to 0 airmasses (a purely imaginary condition, or one which results if the atmosphere is removed), the radiometer sees only the cosmic background and the horn, waveguide, and ground (spillover) thermal noise temperature contributions. We can write, in this case, for the zero airmass intercept value:

$$V_0 = k(T_A + T_C + T_E) \quad (12)$$

where

V_0 = data counts at zero airmass intercept

k = receiver gain, counts/K

T_A = sum of assumed or measured values for horn, waveguide switch, and ground contribution

T_C = cosmic background noise temperature, 2.7 K

T_E = receiver noise temperature, K

Switching to the ambient (“room” temperature) waveguide load results in:

$$V_1 = k(T_P + T_E) \quad (13)$$

where

V_1 = data counts on ambient load

k = receiver gain, counts/K

T_P = physical temperature of ambient load (the waveguide system is assumed to have the same temperature)

T_E = receiver noise temperature, K

A typical value of $T_A + T_C$ (cosmic + horn + ground) is 14 K \pm 1 K based on waveguide measurements and estimates of horn spillover.

From these equations, one can solve for k and T_E . Typical values for some of the above values are:

$$k = 0.004135 \text{ counts/K at 22.235 GHz}$$

$$k = 0.002467 \text{ counts/K at 18.5 GHz}$$

$$T_E \approx 700 \text{ K at 22.235 GHz}$$

$$T_E \approx 900 \text{ K at 18.5 GHz}$$

Switching the receiver to the heated waveguide termination (hot load) allows one to solve for the radiometric noise temperature of the hot load:

$$T_{H,RAD} = \frac{1}{k}(V_2 - V_1) + T_P \quad (14)$$

where

k = gain, counts/K

V_2 = data counts on hot load

V_1 = data counts on ambient load

T_P = physical temperature of ambient load (which equals the radiometric temperature of the ambient load)

Previous measurements of waveguide switch insertion loss and hot load parameters enable one to make preliminary adjustments to the measured physical temperature of the hot load as a first cut at determining its equivalent radiometric noise temperature. A multiplicative factor may be applied to the insertion-loss adjusted value to get the radiometric value as determined by Eq. (14). This method is valid because the physical temperature of the hot load is well regulated, and the correction should remain constant under this condition. Thus, operationally, the hot load radiometric noise temperature may be strictly related to its physical temperature without the necessity of doing tipping curves to continually re-determine receiver gain. Also, a radiometer temperature scale is set up, using the ambient and hot waveguide loads.

Table 2 shows the progressive correction of hot load temperatures from raw to calibrated for a typical hot load physical temperature.

V. Radiosonde Range Delay Measurements

A radiosonde measures pressure, temperature, and relative humidity during its ascent along a nearly vertical path through the atmosphere.

The "wet" range delay may be expressed as:

$$\Delta L = 10^{-6} \int_0^{\infty} N(h) dh \quad (15)$$

where

N = refractivity = $373256.0 \cdot e/T_K^2$

h = height above surface, meters

e = water vapor pressure, millibars (1 mb = 100 N/m²)
 $= 6.1 \cdot 10^B \cdot RH/100$

T_K = temperature, K

$$B = \frac{7.4475T_C}{234.7 + T_C}$$

T_C = temperature, °C

RH = relative humidity, 0 to 100

For each radiosonde launch at Edwards AFB, the range delay was calculated. Typical values for zenith range delay range from 3 cm on a cold, dry winter night to 20 cm on a summer day when the warm air might contain a large amount of water vapor.

A uniform layer of water vapor 3 km thick, relative humidity 50 percent, temperature 7°C, would result in a range delay of 7.13 cm. Typical measurement accuracies of radiosondes are about 10 percent. The radiosonde does not measure liquid water parameters; but since the liquid effect on delay is usually very small, this is not a calibration problem.

VI. WVR Calibration Using EAFB Radiosondes

It was found that only 17 of the many radiosonde measurements made at Edwards AFB could be used in the calibration of the water vapor radiometer. In many cases either the scheduled radiosonde launch was cancelled or the radiometer was not operating properly during a launch.

As stated in Section II, noise temperature saturation effects cause a curved “calibration surface” to result. It is postulated, then, that this surface may be described by:

$$\Delta L = a_0 + a_1 T_{W22} + a_2 T_{W22}^2 + a_3 T_{W18} + a_4 T_{W18}^2 \quad (16)$$

where

ΔL = range delay, cm

T_W = “water” noise temperatures at 22.235 and 18.5 GHz

It is expected that $a_0 = 0.0$ (see Eq. 4).

A plot of the data (T_{W22} vs T_{W18}) shows that the points lie nearly along the theoretical “vapor only” line in Fig. 1. The range of T_{W22} is 24 K to 108 K, and corresponding ΔL 's of 9 cm to 38 cm at a 30-deg elevation angle. This indicates that the measurements did not encompass weather conditions in which liquid water (clouds) was present. Also, it can be seen that it is not possible to accurately describe a surface by a line of experimental points.

In the second-order surface-fit program, various combinations of experimental points and theoretical liquid-only points were used as input data so as to give the surface a 3-dimensional nature. The regression technique uses radiosonde determination of ΔL along with WVR noise temperature values.

Table 3 shows the results of using various combinations of real and theoretical data points. Cases 2 to 6 do not use four data points which appear to be inconsistent with the remaining data.

Referring to Eq. (4), it is seen that, for the case where the noise temperatures are due to vapor and liquid only, there will be no constant term in the calibration equation for ΔL . This is sensible because with no vapor or liquid, there will be no “wet” range delay. For this reason it is probably wise to eliminate Cases 4, 5, and 6 as having an a_0 term which is too large. These three cases show the insensitivity of the first-order terms to different liquid-only points. Of the remaining three cases, Case 1 has a large RMS curve-fit error and a moderately large constant term a_0 . Case 2 has four non-experimental liquid-only points derived from imprecise theory. Case 3 has only two of these points.

Considering the limited amount and scope of the data used, either of the following two expressions could be used as the WVR calibration equation (Cases 2 and 3) (RMS surface-fit errors are below 1 cm in both cases):

$$\begin{aligned} \Delta L = & -0.419 + 0.478T_{W22} - 0.000155T_{W22}^2 \\ & - 0.665T_{W18} - 0.0000696T_{W18}^2 \end{aligned} \quad (17)$$

$$\begin{aligned} \Delta L = & -0.442 + 0.479T_{W22} - 0.000158T_{W22}^2 \\ & - 0.663T_{W18} - 0.0000444T_{W18}^2 \end{aligned} \quad (18)$$

where

ΔL = tropospheric range delay, cm

T_{W22}, T_{W18} = “water” noise temperatures at 22.235 and 18.5 GHz, calculated using the JPL Section 333 data reduction program and the parameters and methods described in this report

The calibration equations above result after the long process of radiometer gain determination and hot load calibration using the tipping curve technique. These calibrations use measurements of waveguide insertion loss, horn beamwidth adjustments, and assumptions of ground spillover contribution. Any change in WVR hardware would make recalibration necessary. The JPL Section 333 WVR data reduction program should be used in conjunction with the given calibration equations. Operators of the same instrument, using a different data reduction method to measure antenna temperature, should use the given calibration equations only with the greatest care.

VII. Remarks

- (1) The WVR calibration Eqs. (17) and (18) result from a limited set of data. The RMS surface-fit errors are below 1 cm, but this may be valid only for vapor-only atmospheric conditions.
- (2) The calibration equations given are not universal. They should be regarded as applicable only to the DSN Water Vapor Radiometer when data is reduced by means of the JPL Section 333 data reduction program.
- (3) Users of the DSN WVR should verify by independent means (radiosondes, VLBI base-line closure, etc.) the accuracy and usefulness of the instrument.
- (4) Further field calibration of the WVR should be done in conjunction with radiosonde measurements. Cloudy weather conditions should be included in these tests.

- (5) Investigation of alternative frequency selection (Ref. 2) should continue in an attempt to improve the inherent accuracy of the two-frequency water vapor radiometry technique to determine tropospheric range delay.
- (6) Further calibration of the WVR should be carried out using refractometers and laser-microwave ranging instrumentation to achieve higher accuracy measurements of ΔL .

Acknowledgment

The authors wish to thank Manuel Franco, Daniel Giles, and Bruce Lyon for their tireless efforts in both operating and maintaining the DSN Water Vapor Radiometer during the numerous field tests at Pt. Mugu, El Monte, Goldstone, and Edwards Air Force Base. Charles Stelzried guided the development of the WVR for the major portion of its early life. His insightful suggestions and assistance regarding operational methods and data reduction techniques are greatly appreciated. Bruce Crow guided WVR development during this last year and brought the WVR to its final configuration.

References

1. Slobin, S. D., and Batelaan, P. D., "DSN Water Vapor Radiometer Development – A Summary of Recent Work, 1976-1977," in *The Deep Space Network Progress Report 42-40*, pp. 71-75, Jet Propulsion Laboratory, Pasadena, Calif., Aug. 15, 1977.
2. Batelaan, P. D., and Slobin, S. D., "DSN Water Vapor Radiometer Development – Recent Work, 1978," in *The Deep Space Network Progress Report 42-48*, pp. 129-135, Jet Propulsion Laboratory, Pasadena, Calif., Dec. 15, 1978.
3. Waters, J. W., *Atmospheric Effects on Radio Wave Phase . . . Water Vapor Emission*, VLA Scientific Memorandum No. 8, National Radio Astronomy Observatory, Sept. 14, 1967.
4. Waters, J. W., *Analysis of Water Vapor Data from the Green Bank Interferometer*, Progress Report No. 1, National Radio Astronomy Observatory, Aug. 31, 1970.
5. Staelin, D. H., "Measurements and Interpretation of the Microwave Spectrum of the Terrestrial Atmosphere near 1-Centimeter Wavelength," *Journal of Geophysical Research*, Vol. 71, No. 12, pp. 2875-2881, June 15, 1966.
6. Goldstein, H., *Propagation of Short Radio Waves*, edited by D. E. Kerr, McGraw-Hill Book Co., New York, 1951.

Table 1. Airmass correction for antenna beamwidth

Horn elevation, deg	22.235 GHz		18.5 GHz	
	Apparent beam elevation, deg	Number of airmasses	Apparent beam elevation, deg	Number of airmasses
90.0	90.0	1.00	90.0	1.01
80.0	78.7	1.02	78.0	1.02
70.0	69.3	1.07	69.0	1.07
60.0	59.5	1.16	59.3	1.16
50.0	49.6	1.31	49.3	1.32
40.0	39.6	1.57	39.3	1.58
30.89	-	-	30.0	2.00
30.59	30.0	2.00	-	-
30.0	29.5	2.03	29.2	2.05
20.0	19.2	3.04	18.8	3.11
15.0	13.9	4.16	13.3	4.36

Table 2. Progressive hot load radiometric noise temperature correction

Frequency, GHz	Typical raw physical temperature, K	Temperature after waveguide loss correction, K	Adjustment factor	Net radiometric hot load noise temperature, K	Total difference, K
22.235	420.83	413.34	0.9729	402.14	18.69
18.5	420.83	410.59	0.9821	403.24	17.59

Table 3. Results of second-order surface fit to EAFB calibration data

Case	Number of points	Number of liquid only	a_0	a_1	a_2	a_3	a_4	RMS error
1	17	7	1.006	0.410	0.000536	-0.639	-0.000538	1.77
2	13	4	-0.419	0.478	-0.000155	-0.665	-0.0000696	0.80
3	13	2	-0.442	0.479	-0.000158	-0.663	-0.0000444	0.85
4	13	1	-4.337	0.675	-0.00128	-1.086	0.00964	0.80
5	13	1	-4.220	0.670	-0.00135	-1.064	0.0110	0.79
6	13	1	-3.952	0.642	-0.000700	-1.026	-0.000768	0.86

Notes:

- Case 1: All radiosonde values and many theoretical points.
Large RMS error of surface fit to data
Liquid-only points have $T_{W22} = 0, 12.5, 25, 37.5, 50, 75, 100$
with $T_{W18} = 0.687 T_{W22}$
- Case 2: Four worst data points of Case 1 eliminated.
Liquid-only points reduced to 0, 25, 50, 100
- Case 3: Liquid-only points 0 and 50
- Case 4: Liquid-only point $T_{W22} = 50, T_{W18} = 34.6$
- Case 5: Liquid-only point $T_{W22} = 50, T_{W18} = 50$
- Case 6: Liquid-only point $T_{W22} = 50, T_{W18} = 25$

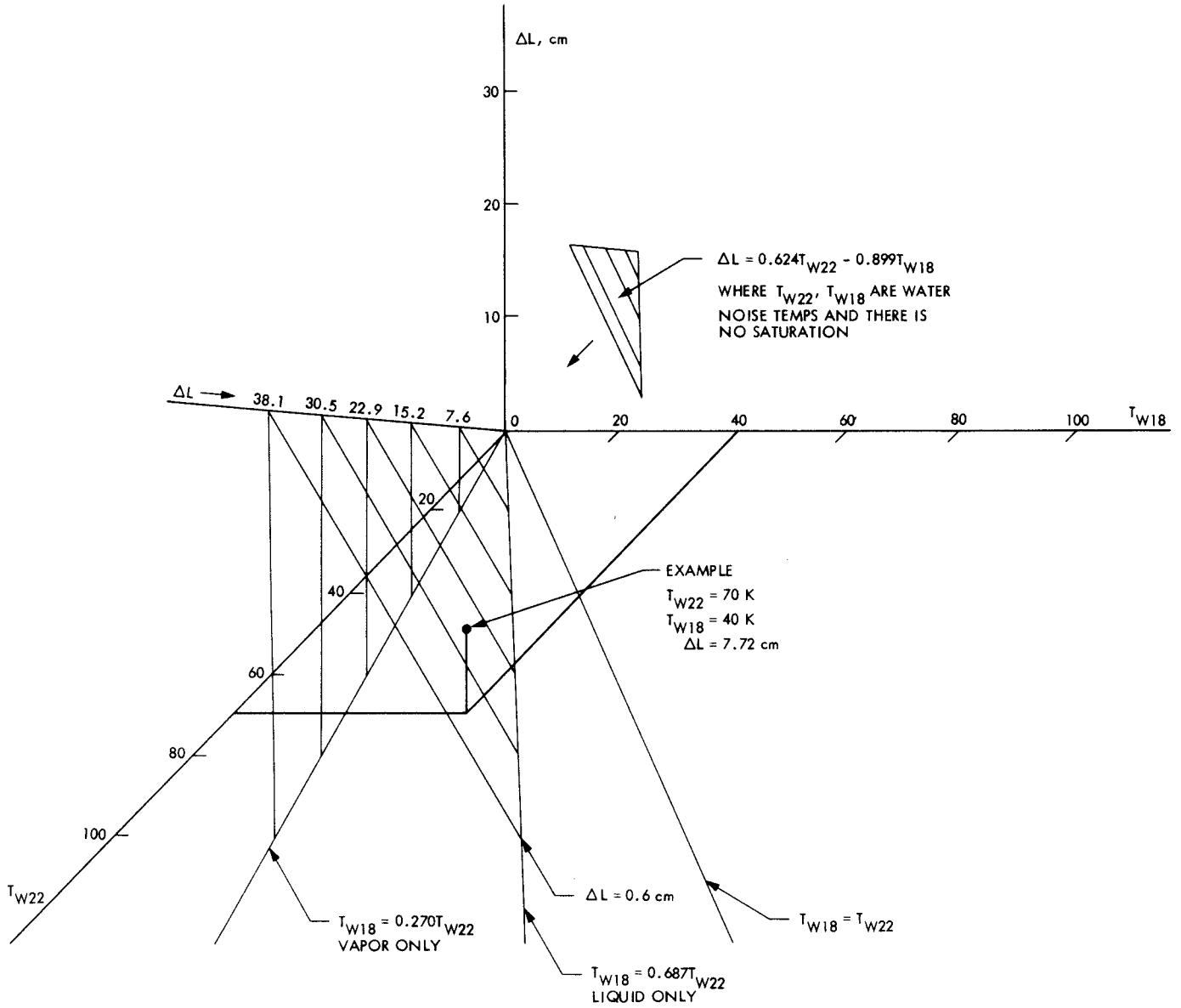


Fig. 1. Tropospheric delay vs brightness temperature

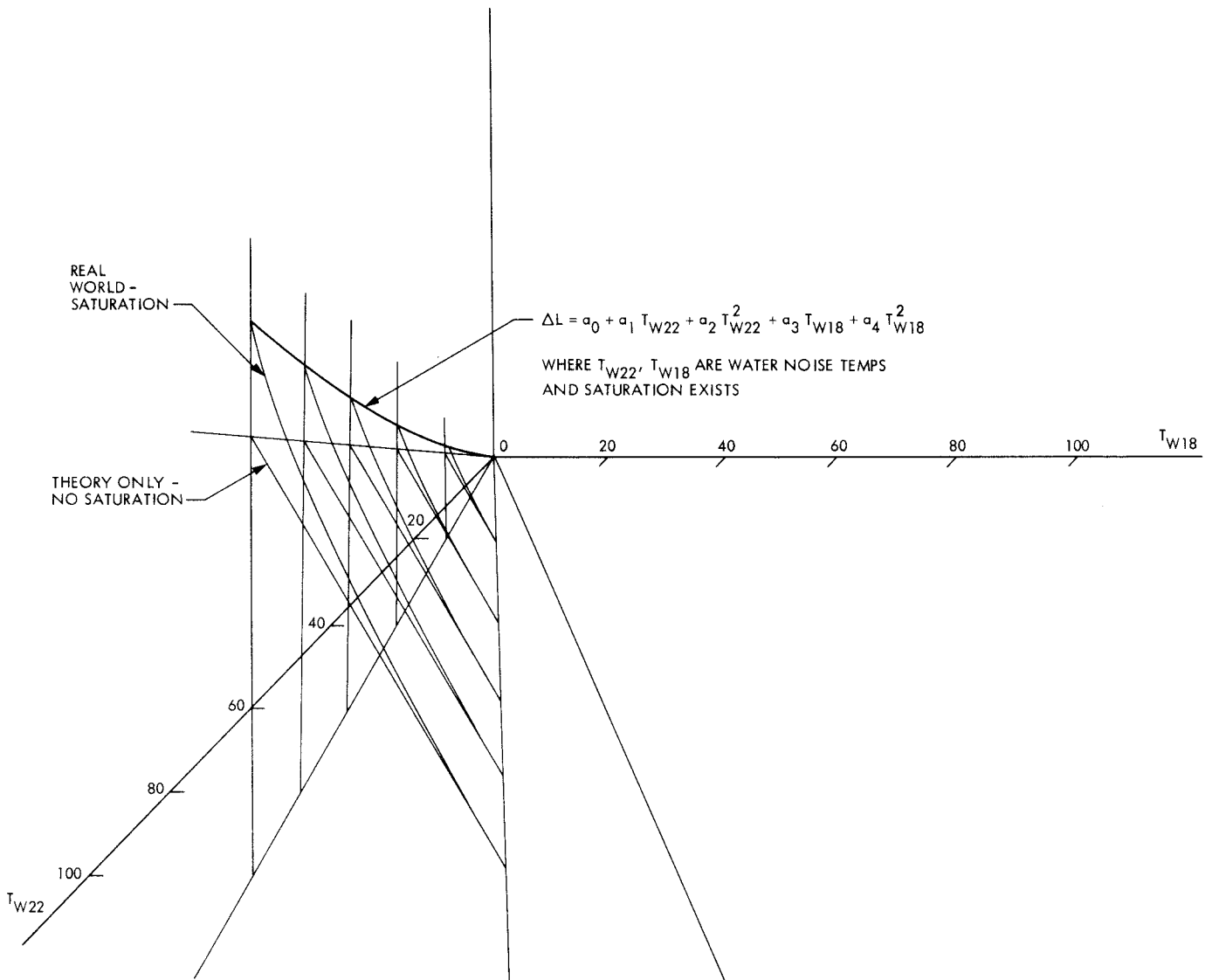


Fig. 2. Tropospheric delay-saturation effect